

Evidence for Two Spectroscopically Different Dimers of Light-Harvesting Complex I from Green Plants[†]

Janne A. Ihalainen,^{*,‡} Bas Gobets,[§] Kinga Sznee,[§] Michela Brazzoli,^{||} Roberta Croce,^{||} Roberto Bassi,^{||} Rienk van Grondelle,[§] Jouko E. I. Korppi-Tommola,[‡] and Jan P. Dekker[§]

Department of Chemistry, University of Jyväskylä, P.O. Box 35, FIN-40351 Jyväskylä, Finland, Department of Physics and Astronomy, Vrije Universiteit, De Boelelaan 1081, 1081 HV Amsterdam, The Netherlands, and Facoltà di Scienze MM. FF. NN., Università di Verona, Strada Le Grazie-Ca' Vignal, 37134 Verona, Italy

Received March 31, 2000; Revised Manuscript Received May 10, 2000

ABSTRACT: A preparation consisting of isolated dimeric peripheral antenna complexes from green plant photosystem I (light-harvesting complex I or LHCI) has been characterized by means of (polarized) steady-state absorption and fluorescence spectroscopy at low temperatures. We show that this preparation can be described reasonably well by a mixture of two types of dimers. In the first dimer about 10% of all Q_y absorption of the chlorophylls arises from two chlorophylls with absorption and emission maxima at about 711 and 733 nm, respectively, whereas in the second about 10% of the absorption arises from two chlorophylls with absorption and emission maxima at about 693 and 702 nm, respectively. The remaining chlorophylls show spectroscopic properties comparable to those of the related peripheral antenna complexes of photosystem II. We attribute the first dimer to a heterodimer of the Lhca1 and Lhca4 proteins and the second to a hetero- or homodimer of the Lhca2 and/or Lhca3 proteins. We suggest that the chlorophylls responsible for the 733 nm emission (F-730) and 702 nm emission (F-702) are excitonically coupled dimers and that F-730 originates from one of the strongest coupled pair of chlorophylls observed in nature.

The principal photosynthetic functions are the harvesting of light energy and the transduction of this energy into ATP and NADPH. These functions are performed in the thylakoid membranes of chloroplasts by four large protein complexes, i.e., the photosystem I (PSI) complex with its associated antenna system (light-harvesting complex I or LHCI), the photosystem II (PSII) complex with its associated antenna system (light-harvesting complex II or LHCII), the cytochrome *b₆f* complex, and the ATP synthase complex (see, e.g., ref 1).

The main task of LHCI is to capture and deliver light energy to the reaction center core complex of PSI, in which the excitation energy is trapped in a form of a stable charge separation. LHCI consists of four polypeptides (called Lhca1–4), which belong to the group of proteins encoded by the Lhc supergene family (2), bind both Chl¹ *a* and Chl *b*, and have protein masses in the range of 20–24 kDa. It was suggested that LHCI forms two kinds of heterodimers in solution, called LHCI-730 and LHCI-680 (2).

The mixture of all LHCI dimers contains on the average eight Chl *a*, two Chl *b*, and two carotenoids per polypeptide (3). All LHCI proteins show considerable sequence homology with those of LHCII (4), and based on the amino acid sequence data and the structural model of LHCII at 3.4 Å resolution (5), it is likely that most of the chlorophylls in LHCI are similarly bound as in LHCII and that both systems should have comparable spectroscopic properties. On the other hand, LHCI contains a number of additional “red” pigments, which absorb (and emit) at low energy and are responsible for its unique long-wavelength emission. Lhca1 and Lhca4 form a heterodimer in solution (6, 7), which gives rise to a 77 K emission band peaking at about 730 nm and is generally referred to as F-730 (4). It was shown that most of the long-wavelength emission originates from Lhca4 (6, 7). Lhca2 and Lhca3 were thought to give rise to 77 K emission peaking at 680 nm (the same maximum as observed for all PSII-associated Chl *a/b* binding proteins) and could therefore be responsible for LHCI-680 (4), but recent experiments suggested that LHCI-680 could also be a product of a monomerization of the LHCI-730 dimer (3). This means that the spectroscopic behavior and function of the Lhca2 and Lhca3 polypeptides remain unresolved.

The number of red chlorophylls and the energy of Q_y states vary from species to species. For example, Pålsson et al. (8) determined that PSI from the cyanobacterium *Synechococcus elongatus* has two red forms, absorbing at 708 and 719 nm. It was estimated that five or six Chl *a* contribute to the C-708 absorption and four or five to C-719. In contrast, PSI from the cyanobacterium *Synechocystis* PCC 6803 contains lower amounts of red pigments. Gobets et al. (9) determined that

[†] The visit of J.A.I. to Amsterdam was supported by the European Science Foundation via the program Biophysics of Photosynthesis. A graduate school scholarship from the University of Jyväskylä is gratefully acknowledged. This work was supported in part by The Netherlands Foundation for Scientific Research (NWO) via the Foundation for Life and Earth Sciences (ALW).

* To whom correspondence should be addressed. Tel: +358 14 602568. Fax: +358 14 602551. E-mail: janne@epr.chem.jyu.fi.

[‡] University of Jyväskylä.

[§] Vrije Universiteit.

^{||} Università di Verona.

¹ Abbreviations: CD, circular dichroism; Chl, chlorophyll; fwhm, full width at half-maximum; LD, linear dichroism; LHC, light-harvesting complex; PS, photosystem.

the red wing of the absorption of *Synechocystis* PCC 6803 is caused by one strongly coupled Chl *a* dimer with an absorption maximum at 708 nm (9). Recently, results from hole-burning spectroscopy suggest that PSI from *Synechocystis* PCC 6803 has also an another red state, located at 714 nm (10). This C-714 species was also suggested to be a strongly coupled Chl *a* dimer.

Despite a number of steady-state and time-resolved spectroscopic studies on isolated dimers consisting of all LHCI proteins (11), or the isolated (12) or reconstituted (13) Lhca1–Lhca4 heterodimer, the picture of the spectroscopic states of LHCI remains unclear. The aim of this study is to determine the spectroscopic states of isolated LHCI dimers consisting of all LHCI proteins and to determine the rather unknown spectroscopic features of Lhca2 and Lhca3. The results identify new absorption and emission bands at 690 and 702 nm, respectively, that are not associated with F-730. These spectroscopic features are tentatively assigned to homo- or heterodimers of Lhca2 and Lhca3.

MATERIALS AND METHODS

Sample Preparation. LHCI complexes were isolated by solubilizing PSI-200 complexes from maize by a treatment using *n*-dodecyl β -D-maltoside (β -DM) and Zwittergent-16 and purified by sucrose density gradient centrifugation according to Croce et al. (11). A preliminary note on the biochemical and pigment analysis of the isolated samples was reported by Croce and Bassi (3), from which it is clear that the purified material contains all four LHCI polypeptides (Lhca1–4), most likely with equal amounts, and consists exclusively of dimers. For low-temperature absorption, CD, and fluorescence measurements the protein complexes were solubilized in 10 mM tricine (pH 7.5), 0.03% β -DM, 0.5 M sucrose, and 75% (v/v) glycerol.

Spectroscopy. The samples were contained in acrylic cuvettes with a 1 cm optical path length (OD, LD, fluorescence) or in a special home-built cuvette with a 0.5 cm path length (CD). For low-temperature measurements the samples were cooled in a liquid nitrogen cryostat (Oxford Instruments, 77 K) or in a helium bath cryostat (Utreks, 4 K). The optical density of the sample measured at 679 nm was about 0.5 cm^{-1} for OD and CD measurements, 0.35 cm^{-1} for LD measurements, and below 0.1 cm^{-1} for fluorescence experiments.

Absorption. Absorption, linear dichroism, and circular dichroism spectra were measured using a home-built spectropolarimeter. The optical bandwidth was varied between 1 and 4.5 nm depending on the measured spectral region. For the LD measurements the protein complexes were embedded in a 6.4% (w/v) solution of commercial gelatin (14, 15) and oriented using a bidirectional compression technique (16) to obtain a compression factor of 1.44 ± 0.1 . Gelatin was used rather than a polyacrylamide gel, to avoid denaturation and pigment loss of proteins due to radical formation during the polymerization of the polyacrylamide gels (17). The absorption spectra of the samples in gelatin were compared with those of samples in buffer to certify the intactness of the proteins.

Fluorescence. Fluorescence emission spectra were measured with a 0.5 m imaging spectrograph (Chromex 500IS) and a CCD camera (Chromex Chromcam I). The spectral

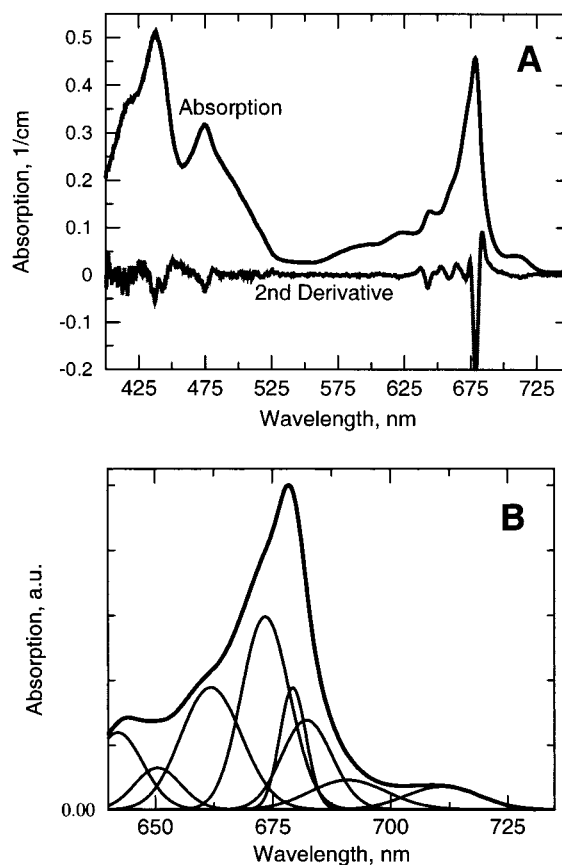


FIGURE 1: Absorption spectrum of LHCI at 6 K and the second derivative of the spectrum (A). The optical bandwidth was 1 nm. Gauss fit from the Q_y region of the absorption spectrum (B).

resolution was varied between 0.25 and 0.5 nm. For broadband excitation a tungsten halogen lamp (Oriel) was used with band-pass filters transmitting at 455 or 475 nm (bandwidth of 20 nm). For narrow band excitation a dye laser (Coherent CR599, dye DCM or pyridine 2) was used which was pumped by an argon ion laser (Coherent Inova 310). The optical bandwidth of the laser was 0.6 nm, and the power was kept below 0.15 mW/cm^2 to limit the effects of hole burning. All emission spectra were corrected for the wavelength dependence of sensitivity of the detection system. Polarizers were used in the excitation and emission beams to obtain polarized fluorescence data.

Fluorescence excitation spectra were recorded on a home-built fluorescence excitation spectrometer. The optical bandwidth of excitation light was 2.5 nm. The wavelength of fluorescence detection was selected with the band-pass filter transmitting at 740 nm (bandwidth of 11 nm). The setup was calibrated using different laser dyes dissolved in ethanol.

RESULTS

Absorption Spectroscopy. Figure 1A shows the absorption spectrum at 5 K of the purified LHCI dimers together with its second derivative. In the Q_y absorption region of the chlorophylls, bands and shoulders can be observed at 643, 650, 660, 672, 679, and \sim 710 nm. The first five bands occur at about the same position as observed before for trimeric and monomeric LHCI complexes (18–21), except that the main Chl *a* transition is observed at 679 nm in LHCI and is red shifted by about 3–5 nm. The red tail of the absorption spectrum reveals a broad band not observed in LHCI

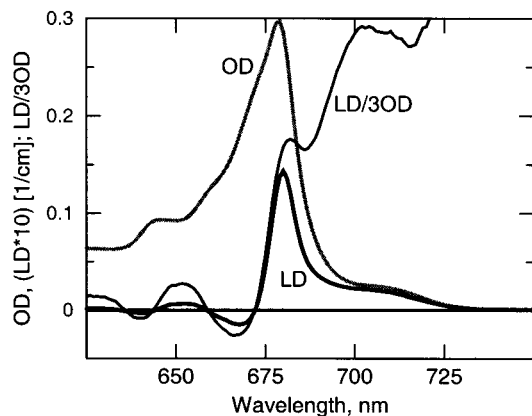


FIGURE 2: OD, LD, and LD/3OD (reduced LD) spectra of LHCI at 77 K. For LD measurement the samples were oriented in a two-dimensionally squeezed gelatin gel (see Materials and Methods). The absorption was measured on unoriented samples and normalized to the OD of the samples used for the LD experiments. To compare the shapes of the OD and LD spectra, the LD spectrum was multiplied by a factor of 10.

peaking at about 710 nm. The Soret bands of Chl *a* and Chl *b* are observed near 437 and 475 nm, respectively, whereas various xanthophylls dominate the absorption between 480 and 520 nm.

In order to get a better idea on the peak wavelength and intensity of the unique long-wavelength band(s) in LHCI, we fitted the O_y region of the 5 K absorption spectrum with Gaussian bands. The result of the Gauss fit analysis (Figure 1B) is a combination of eight bands of which all parameters (peak position, bandwidth, and intensity) have been used as free fit parameters. We note that results from this procedure should be interpreted with much care, because unique fits are seldom found and because there is no good evidence that absorption bands at 5 K have Gaussian shapes. In addition, slightly different fits were found when different starting conditions were used. In general, however, the red-most part of the absorption is described by a single broad band (fwhm 18 nm or 356 cm^{-1}) peaking at 711 nm. The integrated intensity of this band is rather small (about 5% of the intensity of the bands of the fit shown in Figure 1B). In most fits, the next red-most absorption band locates at 693 nm and has a rather similar integrated area as the red-most band at 711 nm.

Linear Dichroism. The Q_y region of the 77 K LD spectrum of LHCI is presented in Figure 2. This spectrum shows a strong positive LD at 680 nm, a weak positive LD around 710 and 650 nm, and a weak negative LD around 668 and 641 nm and is basically similar to the spectra recorded earlier by Tapie et al. (22). The shape of the 680 nm band of LHCI is very similar to that of the main band of CP29 peaking at 675–677 nm (21, 23). The reduced LD spectrum (LD/3OD, dashed line in Figure 2) shows the largest value above 700 nm, a smaller positive value around 680 nm, and a local minimum at 686 nm.

In the case of disk-shaped particles and two-dimensional squeezing, a positive LD implies a larger angle between the transition dipole and the normal of the disk than the magic angle, whereas a negative LD implies a smaller angle than the magic angle (24). Because for most membrane-bound complexes the plane of the disk is parallel to the plane of the membrane, positive and negative LD mean a large and

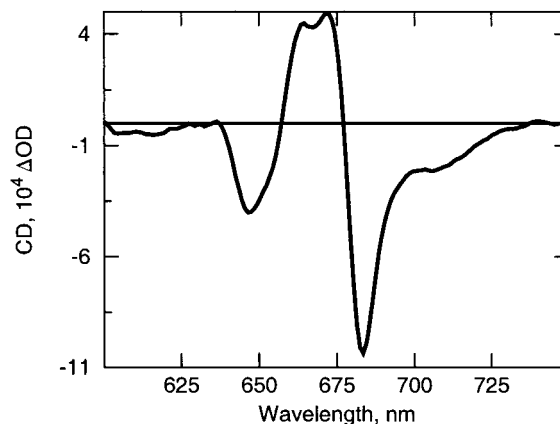


FIGURE 3: Circular dichroism spectrum at 77 K of LHCI, recorded with 1.5 nm optical bandwidth. The spectrum is a mean value of five different measurements. The spectrum is normalized to an OD of 1.0 at 680 nm.

small angle, respectively, between the transition dipole and the normal to the plane of the membrane. These considerations show that the 711, 693, and 680 nm transitions of the two red forms and the main absorption band, respectively, are oriented at increasingly smaller angles with the normal to the plane of the membrane, which are all, however, considerably larger than the magic angle (54.7°).

Circular Dichroism. Figure 3 presents the 77 K CD spectrum of our LHCI preparation. The spectrum consists of positive peaks at 672 and 664 nm and negative peaks and shoulders at ~ 706 , 683, 655, and 647 nm. The general shape of this spectrum is similar to those of other Chl *a/b* binding proteins (18, 21, 25), except that most bands are slightly red shifted and that the red-most band is unique for LHCI. A negative CD signal has also been reported for the long-wavelength chlorophylls in the PSI core complex from *Synechocystis* PCC 6803 (26). The shape of the CD spectrum of our preparation suggests that both long-wavelength absorption bands (711 and 693 nm) give rise to a rather pronounced negative CD at 77 K around 706 nm. The CD signal of the 711 nm band is an order of magnitude larger than the CD signal from isolated Chl *a* (27), which could mean that excitonic interactions between at least two chlorophylls determine the absorption properties of this band. The same is probably true for the 693 nm band, but this is less easy to establish because of the overlap with the negative band at 683 nm caused by “bulk” chlorophylls.

Fluorescence Spectroscopy. Fluorescence emission spectra of LHCI with 455 nm excitation at different temperatures are shown in Figure 4. Emission spectra of the same LHCI preparation at various temperatures above 77 K have been reported and discussed before by Croce et al. (11). The spectra presented in Figure 4 are very similar at the corresponding temperatures and confirm the notion of Croce et al. (11) that the 77 K emission spectrum of our preparation is considerably red shifted compared to that of earlier preparations (12, 28, 29), which was explained by a (partial) monomerization of the LHCI dimers in these earlier preparations, leading to 680 nm emission (3).

The fluorescence emission at 6 K is characterized by two peaks at 733 and 702 nm. The peak at 733 nm is about two times higher than the peak at 702 nm. The latter peak is not observed at all in the Lhca1–4 heterodimer (7) and therefore

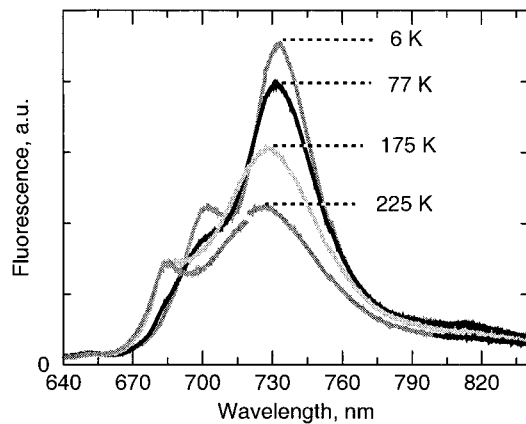


FIGURE 4: Fluorescence emission spectra of LHCI at different temperatures. The sample was excited at 455 nm (optical bandwidth 19 nm), and the spectra were recorded using an optical bandwidth of 0.4 nm. The OD of the sample was 0.06 cm^{-1} at 680 nm. The emission spectra were corrected for the wavelength sensitivity of the detection system.

most likely arises from Lhca2 and/or Lhca3. When the temperature is increased, the main peak stays at about the same position up to about 150 K and then gradually blue shifts to 727 nm at 225 K. Other photosynthetic complexes with “long”-wavelength Chl *a* absorption bands, such as cyanobacterial PSI complexes (8, 10) and the PSI core complex from green plants (11), show essentially the same behavior. The blue shift was considered to be a general feature of all strongly coupled chlorophylls (10). In principle, the blue shift could also be explained by the presence of a number of energetically different red forms in LHCI (11), but the site-selected fluorescence experiments described below will show that there is only one red form in each LHCI dimer.

It is furthermore worthwhile to note that when the temperature is increased from 77 to 175 K, the amplitude of the emission band peaking at about 685 nm rises considerably (Figure 4). We interpret this emission as emission from the main chlorophylls, which are expected to show an increased contribution to the steady-state emission spectrum at higher temperatures. These chlorophylls absorb 3–5 nm more to the red compared to those of the various LHCI complexes (see above) and are therefore also expected to emit 3–5 nm more to the red compared to those systems, which usually show emission maxima around 680 nm. We want to emphasize that the 702 and 685 nm emissions observed by us most likely have a different origin than the 680 nm emission in earlier LHCI preparations and that the F-680 present in these preparations is not observed at all in this work (see, e.g., the 6 K spectrum in Figure 4, where almost no emission is observed at 680 nm).

Site-Selected Fluorescence. Isotropic 6 K fluorescence emission spectra of LHCI obtained with selective excitation at five different wavelengths are shown in Figure 5A. The results show that the intensity ratio of the two main fluorescence bands, $I(702)/I(730)$, varies considerably as a function of excitation wavelength. The relative intensity of the emission at 702 nm increases progressively upon increasing the excitation wavelength to 691 nm but drops steeply upon increasing the excitation wavelength to 701 nm. These results suggest that an absorption band peaking around 691 nm is responsible for the fluorescence at 702 nm and that

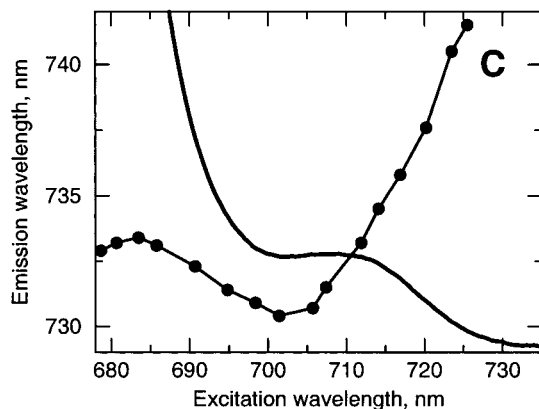
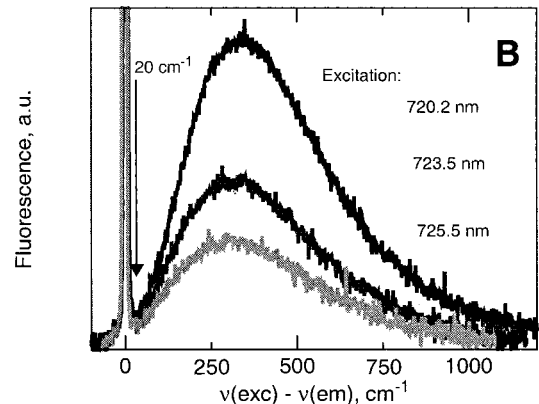
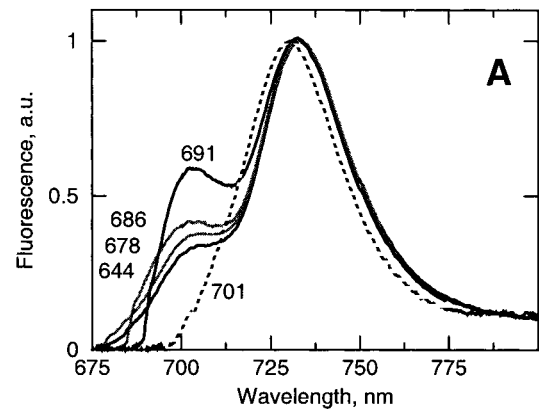


FIGURE 5: Isotropic emission spectra of LHCI at 6 K, laser-excited at 644, 678, 686, 691, and 701 nm (A) or at 720.2, 723.5, and 725.5 nm (B). The OD of the sample was 0.1 cm^{-1} at 680 nm. The spectra in (A) were normalized to the maxima of emission. The spectra in (B) were shifted in such a way that the excitation wavenumbers were at 0 cm^{-1} . (C) Dependence of the fluorescence maximum as a function of excitation wavelength.

excitation at wavelengths above 700 nm preferentially sensitizes the emission band at 730 nm. Emission spectra obtained upon excitation in the far-red edge of the absorption spectrum are shown in Figure 5B.

Figure 5C shows a plot of the excitation wavelength versus the emission maximum (see ref 9 for a detailed explanation of this type of experiment) and reveals that when the excitation wavelength is increased, the maximum of the LHCI emission first shifts to shorter wavelength until a minimal value of 730 nm is observed upon excitation at 702 nm. Then, a further increase of the excitation wavelength results in a shift of the emission maximum to longer wavelengths. For excitation wavelengths longer than 712 nm

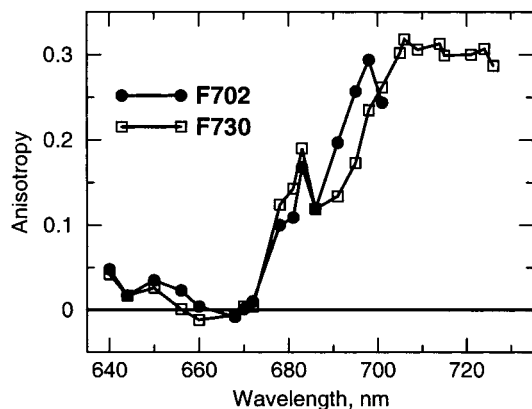


FIGURE 6: Anisotropy of fluorescing components at 702 nm (F-702) and at 732 nm (F-730) in LHCI at 6 K.

a linear relation between emission and excitation wavelengths is observed with a slope of about 0.6–0.7. This slope (abbreviated as s in the following) is similar to that observed in PSI complexes (~ 0.6 in *Synechocystis* and ~ 0.77 in PSI-200; 9) and suggests that for the long-wavelength absorbing species the inhomogeneous bandwidth (Γ_i) contributes more to the overall width of the absorption band than the homogeneous bandwidth (Γ_h). From the Gaussian fit of Figure 1B a value of 356 cm^{-1} is estimated for total fwhm. According to the equations in ref 9, the values of the overall width and of s lead to values of $\sim 210\text{ cm}^{-1}$ for Γ_h and $\sim 290\text{ cm}^{-1}$ for Γ_i in LHCI. In PSI-200 Γ_h and Γ_i were estimated to be about 200 and 360 cm^{-1} , respectively (9).

The results presented in Figure 5C also give an independent determination of the peak position of the complete absorption band of this group of long-wavelength pigments. According to Gobets et al. (9) this peak position (designated as λ_0) can be estimated according to

$$\lambda_0 = \lambda_{\text{ex}} - \frac{\lambda_{\text{em}} - \lambda_{0,\text{em}}}{s}$$

in which λ_{ex} and λ_{em} are the excitation and emission wavelengths, respectively, s is the slope ($d\lambda_{\text{em}}/d\lambda_{\text{ex}}$), and $\lambda_{0,\text{em}}$ is the emission maximum of the nonselectively excited spectrum. With $\lambda_{\text{ex}} = 711\text{ nm}$, λ_{em} appeared to be identical to $\lambda_{0,\text{em}}$ (Figure 5). This observation confirms the results of the analysis of the 4 K absorption spectrum (Figure 1) that the absorption of red-most long-wavelength pigments of LHCI peaks at 711 nm.

Fluorescence anisotropy values as a function of excitation wavelength are shown in Figure 6 for both fluorescing components of LHCI (F-730 and F-702). These values give information on the angle between the absorbing and emitting dipoles and can theoretically vary between 0.4 and -0.2 for parallel and perpendicular dipoles, respectively, although due to imperfections of the equipment the maximal values are often not reached. For F-730 a maximum anisotropy value of about 0.32 is reached upon excitation at wavelengths longer than about 705 nm, whereas for F-702 the highest anisotropy values are observed at excitation wavelengths longer than 695 nm. These results suggest that energy transfer to F-730 and F-702 is negligible above 705 and 695 nm, respectively, although the rather unlikely situation of energy transfer between identically oriented transitions can formally not be excluded. Notable is that both emitting components

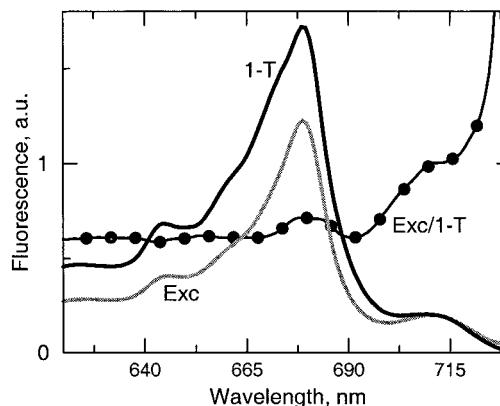


FIGURE 7: Isotropic fluorescence excitation spectrum (upper curve) and 1-minus-transmission spectrum ($1 - T$, lower curve) of LHCI at 6 K. The detection wavelength was 740 nm. The optical bandwidth was 2.5 nm in excitation and 11 nm in emission. The OD of the sample was 0.05 cm^{-1} at 680 nm. The solid line with circles represents the ratio of the $1 - T$ and excitation spectra.

show an anisotropy maximum with about 682 nm excitation and that a maximum at this position is also observed in the reduced LD spectrum (Figure 2).

Fluorescence Excitation. Figure 7 (solid line) shows the excitation spectrum of the emission at 740 nm (fwhm 11 nm) of the LHCI dimers at 6 K. This emission is mainly due to F-730, but not exclusively, because vibrational bands of F-702 are also expected to be present at about 740 nm. The ratio between the excitation and 1-minus-transmission ($1 - T$) spectra, normalized at 711 nm, is shown as a solid line with circles. This ratio is expected to be 1 if all absorbed excitation energy is transferred to lowest energy pigments (the fluorescent state) and lower than 1 if the lower energy pigments cannot be reached by all absorbing pigments.

Between 620 and 670 nm the spectrum remains constant with a value of about 0.58. This ratio is slightly higher than 0.5 and can qualitatively be explained by complete transfer to F-730 in half of the complexes and a small contribution of F-702 vibrational bands at 740 nm in the other half of the complexes. A local maximum in the excitation/ $1 - T$ spectrum locates at 681 nm. A minimum of this spectrum locates between 685 and 695 nm, at which excitation wavelengths the fluorescence at 702 nm increases with respect to the F-730 fluorescence (Figure 5A). Thus, at this wavelength region more absorbing chlorophyll molecules give rise to F-702 emission than to F-730 emission. Between 695 and 710 nm the ratio becomes 1, which shows that only in the red tail of the absorption spectrum do all absorbed photons emit around 740 nm. The excitation spectrum shows higher values than the $1 - T$ spectrum at excitation wavelengths longer than 717 nm, at which wavelengths scattering of the excitation light becomes detectable.

DISCUSSION

Origin of F-730 and F-702. The results in this work indicate the presence of two emitting components at low temperatures in our preparation of dimeric LHCI. The first is the well-known F-730 emission band, from which there is conclusive evidence that it is caused by the Lhca1–Lhca4 heterodimer (see, e.g., ref 7). The second is the up to now unknown component that fluoresces maximally at 702 nm at low temperatures and that we have denoted as F-702 in

this paper. On the basis of its properties (discussed in detail below) and on the presence of Lhca2 and Lhca3 in the dimers of our investigation (3), we propose that F-702 is caused by a hetero- or homodimer of Lhca2 and Lhca3.

There is not much doubt that at 5 K F-730 originates from a broad absorption band (fwhm 18 nm) that peaks at 711 nm (Figure 1) and is oriented almost parallel to the membrane plane (Figure 2). On the basis of the absorption properties we estimate that the absorption band responsible for F-730 generates about 5% of the total absorption in the Q_y region. If half of the total Q_y absorption arises from the Lhca1–Lhca4 dimer, then about 10% of the absorption of Lhca1/4 occurs in the 711 nm band, which combined with the idea that isolated LHCI binds 20 Chl *a* + *b* per dimer (3) suggests that it arises from two monomeric chlorophylls or one dimeric chlorophyll. Indications for a dimeric organization of long-wavelength chlorophylls have been found in PSI from the cyanobacterium *Synechocystis* PCC 6803 (9, 10). A dimeric organization of the two chlorophylls responsible for F-730 in Lhca1/4 provides the most straightforward explanation for the absence of energy transfer above 705 nm (Figure 6). The CD spectrum (Figure 3) suggests these chlorophylls to form an excitonically coupled dimer.

The peak wavelength of the absorption band responsible for the F-702 emission is less easy to establish because of the overlap with other spectral components. However, the relative occurrence of F-702 in the site-selected emission spectra (Figure 5) and the dip in the excitation spectrum of the F-730 emission (Figure 7) consistently indicate that the peak wavelength of the component responsible for the F-702 emission should be located at about 690–695 nm. This wavelength is shorter than that of the primary electron donor of PSI (P700), and therefore this component does formally not belong to the group of red chlorophylls in PSI, because usually only those chlorophylls are included in this group that absorb at longer wavelength than P700. Within the family of Chl *a/b* binding proteins, however, this component is special, because its absorption maximum is considerably red shifted compared to the Chl *a/b* binding proteins associated with PSII, which all have a red-most absorption band peaking at about 680 nm at 4 K. In the green algae *Chlamydomonas reinhardtii*, however, an emission maximum at 705 nm has been observed (30), and it is possible that the spectral component responsible for this emission band is similar to the one responsible for F-702 in plants.

The fact that F-702 gives a rather pronounced contribution to the steady-state emission spectrum (Figure 4) suggests that F-702 and F-730 are not, or only weakly, connected by energy transfer in the LHCI preparation. Combined with the complete absence of F-702 in the emission spectrum of the Lhca1–Lhca4 dimer (6, 7) and the presence of Lhca2 and Lhca3 in our material, the conclusion is justified that F-702 arises from a dimer consisting of Lhca2 and/or Lhca3. We note that, apart from the peak wavelengths of absorption and emission, most spectroscopic properties (LD, CD, fluorescence anisotropy) are quite similar for F-702 and F-730, suggesting a similar origin for both long-wavelength spectral forms. We also note that in PSI-200 complexes the 702 nm emission has never been observed. This suggests that in PSI-200, where several LHCI dimers are firmly connected to the PSI core complex, efficient (downhill) excitation energy transfer occurs from the red chlorophylls in the Lhca2/3

dimer to either F-730 in the Lhca1/4 dimer, F-720 in the PSI core complex, or directly to the primary donor P700 in the core complex.

Nature of the Chlorophylls Responsible for F-730. On the basis of site-selective fluorescence measurements on PSI-200 particles from spinach, we have previously suggested that the red-most absorption band in these particles peaks at 716 nm and has a bandwidth of about 400 cm^{-1} (9). This peak wavelength was considered to be an upper limit, since energy transfer from the long-wavelength chlorophylls in the PSI core to those of LHCI (26) and/or a possible energy transfer between two Lhca1/4 dimers would shift the peak to shorter wavelengths. The results in the present contribution (a peak wavelength at 711 nm and a bandwidth of 356 cm^{-1} for F-730) may suggest that the maximum of the F-730 absorption band has indeed been overestimated in PSI-200. However, the possibility that the spectroscopic properties of F-730 differ somewhat between PSI-200 and isolated LHCI should also be taken into account. Indications for different emission properties of F-730 in isolated LHCI dimers and in PSI-200 have been reported by Knoetzel et al. (31) and were also observed by us (J. Ihalainen, unpublished observations).

It has recently been suggested that the red tail of the absorption spectrum of the LHCI dimers can be described reasonably well by three red forms connected by energy transfer and peaking near 701, 715, and 726 nm and that the spectral form peaking at 726 nm would be responsible for the emission at 733 nm (11). The results in Figures 5 and 6 indicate, however, that this description cannot be correct. The anisotropy of the emission is maximal for all excitation wavelengths longer than about 710 nm (Figure 6). This means that if there were more than one band connected by energy transfer, they must have exactly the same orientation of their Q_y transitions, which is very unlikely. But even this case can be excluded by the results of our site-selected emission experiments, because excitation at 726 nm (the peak wavelength of the red-most form proposed in ref 11) does not result in an average emission peak at 733 nm but in a clearly red-shifted maximum at 742 nm (Figure 5C). We conclude that the spectral forms proposed in ref 11 arise from the same set of inhomogeneously broadened spectral bands and thus that the absorption and emission spectra of the long-wavelength chlorophylls of the Lhca1/4 dimer originate from one set of coupled chlorophylls absorbing and emitting at 711 and 733 nm, respectively.

These results imply that the Stokes shift of the chlorophylls responsible for F-730 is extremely large (22 nm or 420 cm^{-1}) and even larger than, for instance, the red-absorbing chlorophylls in PSI from *Synechocystis* PCC 6803, for which a Stokes shift of 160 cm^{-1} (or 8 nm) has been suggested by Rätsep et al. (10). These authors also suggested that, for the explanation of the 160 cm^{-1} Stokes shift, not only the coupling to the usually observed phonons at $\sim 20\text{ cm}^{-1}$ should be taken into account but also a coupling to higher frequency phonons at $\sim 100\text{ cm}^{-1}$. We agree with this suggestion, except that the higher energy phonons must occur at considerably higher frequency in the Lhca1/4 dimer from spinach than in PSI from *Synechocystis*, as can be concluded from the site-selected emission spectra shown in Figure 5B. We note that with the available evidence we cannot estimate

the Huang–Rhys factors of the two types of coupling phonons and that the spectra in Figure 5B, obtained upon excitation in the red edge of the absorption spectrum, are very different from those recorded upon site-selective excitation in the red edge of the absorption spectra of other chlorophyll–protein complexes. Selective excitation of weakly coupled chlorophylls, such as those of trimeric LHCII (32), the PSII RC complex (33), or CP43 (17), consistently revealed a very pronounced $\sim 20\text{ cm}^{-1}$ mode, a large number of vibrational zero-phonon lines, and, in case of the latter two complexes, a very weak second mode at $\sim 80\text{ cm}^{-1}$. More strongly coupled chlorophylls, such as the red PSI chlorophylls from *Synechocystis* and the bacteriochlorophylls of the LH1 complexes from photosynthetic purple bacteria, revealed dominant “second” modes at about 80 cm^{-1} for LH1 (34) and 150 cm^{-1} for PSI from *Synechocystis* (9). Recent experiments showed that in both LH1 (M. Wendling, unpublished observations) and PSI from *Synechocystis* (B. Gobets, unpublished observations) weak 20 cm^{-1} modes still can be observed in these systems but that vibrational fine structure remained beyond detection. Thus, the tendency seems to be that an increase of the coupling increases the intensity and red shift of the second mode and decreases the intensities of the 20 cm^{-1} mode and of the zero-phonon line.

Our red-most excitation of the Lhca1/4 dimer from spinach revealed a very pronounced second mode at about 300 cm^{-1} , but virtually no 20 cm^{-1} mode (Figure 5B) and vibrational fine structure, and thus points to a situation of even stronger coupling than in PSI from *Synechocystis* or in purple bacterial LH1. In the latter systems, the red states have been suggested to have significant charge-transfer character (see, e.g., refs 10 and 35), and it is therefore not unreasonable to assume that also the red state in the Lhca1/4 dimer has considerable charge-transfer character. Stark spectroscopy will be performed to shed more light on this issue.

ACKNOWLEDGMENT

The authors thank Dr. Herbert van Amerongen and Mr. Juha Linnanto for valuable discussions.

REFERENCES

1. Wollman, F.-A., Minai, L., and Nechusthai, R. (1999) *Biochim. Biophys. Acta* 1411, 21–85.
2. Jansson, S. (1999) *Trends Plant Sci.* 4, 236–240.
3. Croce, R., and Bassi, R. (1998) In *Photosynthesis: Mechanisms and Effects* (Garab, G., Ed.) Vol. I, pp 421–424, Kluwer Academic Publishers, Amsterdam, The Netherlands.
4. Jansson, S. (1994) *Biochim. Biophys. Acta* 1184, 1–19.
5. Kühlbrandt, W., Wang, D. N., and Fujiyoshi, Y. (1994) *Nature* 367, 614–621.
6. Knoetzel, J., Svendsen, I., and Simpson, D. J. (1992) *Eur. J. Biochem.* 206, 209–215.
7. Schmid, V. H. R., Cammarata, K. V., Bruns, B. U., and Schmidt, G. W. (1997) *Proc. Natl. Acad. Sci. U.S.A.* 94, 7667–7672.
8. Pålsson, L.-O., Flemming, C., Gobets, B., van Grondelle, R., Dekker, J. P., and Schlodder, E. (1998) *Biophys. J.* 74, 2611–2622.
9. Gobets, B., van Amerongen, H., Monshouwer, R., Kruij, J., Rögner, M., van Grondelle, R., and Dekker, J. P. (1994) *Biochim. Biophys. Acta* 1188, 75–85.
10. Rätsep, M., Johnson, T. W., Chitnis, P. R., and Small, G. J. (2000) *J. Phys. Chem. B* 104, 836–847.
11. Croce, R., Zucchelli, G., Garlaschi, F. M., and Jennings, R. C. (1998) *Biochemistry* 37, 17355–17360.
12. Pålsson, L.-O., Tjus, S. E., Andersson, B., and Gillbro, T. (1995) *Biochim. Biophys. Acta* 1230, 1–9.
13. Melkozernov, A. N., Schmid, V. H. R., Schmidt, G. W., and Blankenship, R. E. (1998) *J. Phys. Chem. B* 102, 8183–8189.
14. Otte, S. C. M. (1992) Doctoral Thesis, University of Leiden, The Netherlands.
15. Kleima, F. J. (1999) Doctoral Thesis, Free University of Amsterdam, The Netherlands.
16. Abdourakhmanov, I. A., Ganago, A. O., Erokhin, Y. E., Solov'ev, A. A., and Chugunov, V. A. (1979) *Biochim. Biophys. Acta* 546, 183–186.
17. Groot, M.-L., Frese, R. N., de Weerd, F. L., Bromek, K., Pettersson, Å., Peterman, E. J. G., van Stokkum, I. H. M., van Grondelle, R., and Dekker, J. P. (1999) *Biophys. J.* 77, 3328–3340.
18. Hemelrijk, P. W., Kwa, S. L. S., van Grondelle, R., and Dekker, J. P. (1992) *Biochim. Biophys. Acta* 1098, 159–166.
19. Nussberger, S., Dekker, J. P., Kühlbrandt, W., van Bolhuis, B. M., van Grondelle, R., and van Amerongen, H. (1994) *Biochemistry* 33, 14775–14783.
20. Zucchelli, G., Dainese, P., Jennings, R. C., Breton, J., Garlaschi, F. M., and Bassi, R. (1994) *Biochemistry* 33, 8982–8990.
21. Pascal, A., Gradinaru, C., Wacker, U., Peterman, E., Calkoen, F., Irrgang, K.-D., Horton, P., Renger, G., van Grondelle, R., Robert, B., and van Amerongen, H. (1999) *Eur. J. Biochem.* 262, 817–823.
22. Tapie, P., Choquet, Y., Breton, J., Delepelaire, P., and Wollman, F.-A. (1984) *Biochim. Biophys. Acta* 767, 57–69.
23. Simonetto, R., Crimi, M., Sandonà, D., Croce, R., Cinque, G., Breton, J., and Bassi, R. (1999) *Biochemistry* 38, 12974–12983.
24. Van Amerongen, H., Vasmel, H., and van Grondelle, R. (1988) *Biophys. J.* 54, 65–76.
25. Van Amerongen, H., van Bolhuis, B. M., Betts, S. D., Mei, R., van Grondelle, R., Yocum, C. F., and Dekker, J. P. (1994) *Biochim. Biophys. Acta* 1188, 227–234.
26. Van der Lee, J., Bald, D., Kwa, S. L. S., van Grondelle, R., Rögner, M., and Dekker, J. P. (1993) *Photosynth. Res.* 35, 311–321.
27. Kwa, S. L. S., Völker, S., Tilly, N. T., van Grondelle, R., and Dekker, J. P. (1994) *Photochem. Photobiol.* 59, 219–228.
28. Mukerji, I., and Sauer, K. (1993) *Biochim. Biophys. Acta* 1142, 311–320.
29. Tjus, S. E., Roobol-Boza, M., Pålsson, L.-O., and Andersson, B. (1995) *Photosynth. Res.* 45, 41–49.
30. Bassi, R., Soen, S. Y., Frank, G., Zuber, H., and Rochaix, J.-D. 1992 *J. Biol. Chem.* 267, 25714–25721.
31. Knoetzel, J., Bossmann, B., and Grimme, L. H. (1998) *FEBS Lett.* 436, 339–342.
32. Peterman, E. J. G., Pullerits, T., van Grondelle, R., and van Amerongen, H. (1997) *J. Phys. Chem. B* 101, 4448–4457.
33. Peterman, E. J. G., van Amerongen, H., van Grondelle, R., and Dekker, J. P. (1998) *Proc. Natl. Acad. Sci. U.S.A.* 95, 6128–6133.
34. Van Mourik, F., Visschers, R. W., and van Grondelle, R. (1992) *Chem. Phys. Lett.* 195, 1–7.
35. Sundström, V., Pullerits, T., and van Grondelle, R. (1999) *J. Phys. Chem. B* 103, 2327–2346.